





## Efficient computation by molecular competition networks

Haoxiao Cai , Xiaoran Zhang, Rong Qiao, Xiaowo Wang \*, and Lei Wei †

Ministry of Education Key Laboratory of Bioinformatics, Center for Synthetic and Systems Biology, Beijing National Research Center for Information Science and Technology, Department of Automation, Tsinghua University, Beijing 100084, China

 (Received 25 August 2023; revised 5 February 2024; accepted 1 August 2024; published 22 August 2024)

Most biomolecular systems exhibit computation abilities, which are often achieved through complex networks such as signal transduction networks. Particularly, molecular competition in these networks can introduce crosstalk and serve as a hidden layer for cellular information processing. Despite the increasing evidence of competition contributing to efficient cellular computation, how this occurs and the extent of computational capacity it confers remain elusive. In this study, we introduced a mathematical model for molecular competition networks (MCNs) and employed a machine learning-based optimization method to explore their computational capacity. Our findings revealed that MCNs, when compared to their noncompetitive counterparts, demonstrate superior performance in both discrete decision-making and analog computation tasks. Furthermore, we highlighted the nonnegligible role of weak interactions and limited amounts of resources and examined how biological constraints influence the computational capacity of MCNs. The study suggested the potential of MCNs as efficient computational structures and provided new insights into cellular information processing.

DOI: [10.1103/PhysRevResearch.6.033208](https://doi.org/10.1103/PhysRevResearch.6.033208)

### I. INTRODUCTION

Life senses and processes diverse signals to adapt to continuously changing environments, using minimal energy and molecular resources [1]. Even single cells can exhibit intricate computational behaviors, as observed in phenomena like bacterial chemotaxis [2] and cell differentiation [3]. Unveiling the general mechanisms of such computational behaviors can not only help understand how cells efficiently process information but also inspire the design of artificial biological systems and *in silico* computation modules.

Cells process information with biomolecular networks, where different molecules often exhibit promiscuous interactions. Competition for limited molecules thus arises, introducing crosstalk among molecules without direct interactions and forming a hidden regulation layer of the networks [4]. Some studies suggested that the promiscuous interactions in signal transduction networks may introduce subtle regulation or enhance signal processing capacity [5–7]. By modeling the bone morphogenetic protein (BMP) pathway quantitatively, researchers found that the promiscuous interactions in the BMP pathway can serve as a signal processing module [8]. The response function of the BMP pathway varies based on cell-type-specific receptor levels [8], enabling context-dependent combinatorial logic [9] and cell addressing [10].

Theoretical studies have been carried out to uncover the role of molecular competition in cellular computation. Competition accompanied by positive feedback was proved to be able to recognize general patterns through a winner-take-all (WTA) manner [11]. By modeling a large-scale ligand-receptor system as a dynamic multiple inputs-multiple outputs system, researchers found that the system can efficiently sense the concentration of ligands with the temporal sequence of ligand-receptor binding and unbinding events [12]. Some recent research conceptualized the computation role of competitive protein dimerization networks as “computational capability” and tried to reveal the principles behind the computation [13,14].

However, these studies focused on either specific biological systems or specific variants of competition. The characterization of molecular competition networks (MCNs) as a generalized computational module has not yet been revealed. In this study, we raised several questions originating in but transcending cell biology: whether MCNs can serve as universal computational modules, and if so, how strong their computational capability is and what are the key factors that guarantee the capability? We formulated a general, abstract, minimal mathematical model of abstract MCN and employed a machine learning-based optimization method to explore the computational capability of MCNs. The results indicated that MCNs outperformed linear and noncompetition models in both discrete decision-making and analog computation tasks. Limited amounts of competed-for resources and promiscuous interactions are crucial for the computational capability. Weak binding affinities are non-negligible in many cases, especially for implementing complex computations. These findings highlighted the critical role of competition in cellular computation and suggested that MCNs can benefit the construction of efficient computation modules both *in vivo* and *in silico*.

\*Contact author: [xwwang@tsinghua.edu.cn](mailto:xwwang@tsinghua.edu.cn)

†Contact author: [weilei92@tsinghua.edu.cn](mailto:weilei92@tsinghua.edu.cn)

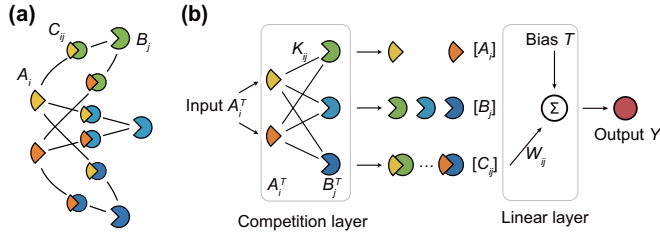


FIG. 1. (a) The schematic diagram of the promiscuous binding molecular system. (b) The illustration of molecular competition networks (MCNs), which consists of a competition layer and a linear layer.

## II. THE MATHEMATICAL MODEL OF MCNs

Competition is widespread in cells, taking part in various biological processes, such as transcription, post-transcription, and translation [4]. We previously proposed a minimal model to illustrate the competition among competitors for one species of resources [4]. Here, we extended the model to describe the competition among multiple competitors  $A_i$  ( $i = 1, \dots, n_A$ ) for multiple resources  $B_j$  ( $j = 1, \dots, n_B$ ) [Fig. 1(a)]. The system is similar to a bipartite graph, which is the shared structure in many biological molecular competition systems, such as the BMP pathway [8] and the competing endogenous RNA (ceRNA) network [15], both of which can be regarded as multicompetitor multiresource systems. The bipartite graph structure is also employed by the restricted Boltzmann machine (RBM), a famous artificial neural network (ANN) [16].

We considered MCNs as a general complex network structure and thus proposed a minimal model where reactions other than binding and dissociation are not considered and focused on the equilibrium state of the system. This simplification can well fit real biological scenarios when the interactions operate much faster than other reactions, and is widely used in studying various biological systems [17–19]. Such a model can also be suitable for describing many other scenarios, such as chemical reaction systems in which thermodynamic equilibrium prevails, as well as *in silico* computations.

In this model, each  $A_i$  can reversibly bind with each  $B_j$  to form complexes  $C_{ij}$ ,



We used  $[A_i]$ ,  $[B_j]$ , and  $[C_{ij}]$  to denote the equilibrium concentration of  $A_i$ ,  $B_j$ , and  $C_{ij}$ . When the system comes to equilibrium, we have

$$[C_{ij}] = K_{ij}[A_i][B_j], \quad (2)$$

where  $K_{ij}$  is the equilibrium constant. Since the amount of molecules can hardly be regarded as unlimited in cells, we used  $A_i^T$ ,  $B_j^T$  to denote the total concentration of  $A_i$ ,  $B_j$ . By the conservation of mass, we got

$$A_i^T = [A_i] + \sum_j [C_{ij}], \quad (3)$$

$$B_j^T = [B_j] + \sum_i [C_{ij}]. \quad (4)$$

Taking  $A_i^T$  as inputs and the equilibrium concentrations as outputs, the competition system performs like a computation

module with parameters  $K_{ij}$  and  $B_j^T$ . We named it a “competition layer.”

We supposed each complex molecule  $C_{ij}$  has a linear effect on the downstream signal  $Y$  with weights  $W_{ij}$ ,

$$Y = \sum_{i,j} W_{ij}[C_{ij}] + b, \quad (5)$$

where  $b$  is an offset. We named this a “linear layer.” Here, a positive  $W_{ij}$  means that  $C_{ij}$  can activate  $Y$ , and *vice versa*. It should be noticed that the linear layer is a simplified model to describe the effect of  $C_{ij}$  to the final output without synergistic or antagonistic effects, as we here focused on the computational capacity contributed by MCNs. This assumption was adopted in previous studies to describe the phosphorylation of SMAD proteins in BMP pathways [8]. In other biological scenarios such as the Hill equation, the relationship between  $[C_{ij}]$  and  $Y$  may be nonlinear, and we can modify Eq. (5) to describe them.

A competition layer and a linear layer compose the minimal computational model of MCNs [Fig. 1(b)]:

$$Y = \text{linear}(\text{competition}(A^T | B^T, \mathbf{K}) | \mathbf{W}, b). \quad (6)$$

It should be noticed that the competition layer with  $n_B > 1$  is much more complicated than that with  $n_B = 1$  which we studied before [4]. Considering Eqs. (2)–(4) as an equation set, the order of any variable is  $\binom{n_A+n_B}{n_A}$ , which dramatically increases with  $n_A$  when  $n_B > 1$ . This makes the system hard to analyze. We proposed an iterative method for solving the steady state of the competition layer.

The functions of a biological network highly depend on its parameter configurations. Numerous studies have employed methods such as parameter scanning [4] and random sampling [20] to elucidate the functions of these networks. However, these exploration-based approaches tend to be inefficient in high-dimensional parameter spaces. Recent advancements in machine learning, particularly physics-informed neural networks (PINNs), have shown considerable potential in solving both forward and inverse problems in dynamic systems [21,22]. As a result, these methods are increasingly utilized for parameter optimization in biological systems [23–25]. Here, we proposed a learning-based approach that first defines all functional targets as shown in Eq. (6), then optimizes the parameters to assess whether these targets can be achieved.

Details of the iterative method and the parameter optimization technique are provided in the Supplemental Material [26]. The code is available in Ref. [27].

## III. THE COMPUTATIONAL CAPACITY OF MCNs

Here we defined the computational capacity of a model as its ability to fit different functions. Discrete decision making such as Boolean operations are fundamental functions in general information processing, DNA computing, and synthetic gene circuits [11,28,29]. The information processing of cells was also simplified as Boolean operations in many studies [30,31]. Thus, we examined all 2-input Boolean functions, 3-input Boolean functions, and 2-input 3-quantized Boolean functions as tasks to evaluate the computational capacity of MCNs [Fig. 2(a)]. For 2-input Boolean functions, we considered the input  $A_i^T$  at  $10^{-1}$  (low) or  $10^1$  (high), forming

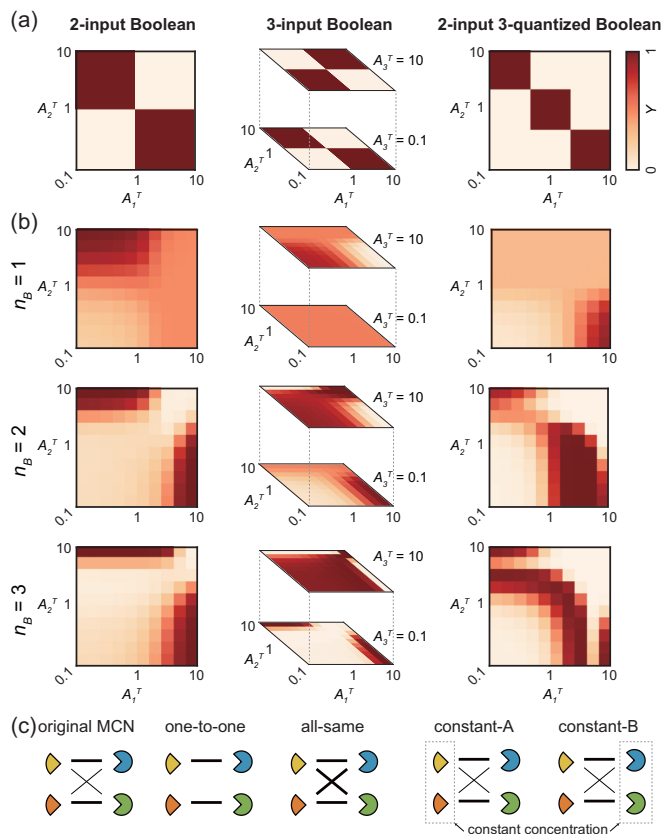


FIG. 2. (a) Examples of target functions in different tasks. (b) The outputs of MCNs trained by the corresponding targets function in (a), visualized on a  $10 \times 10$  grid at the logarithmic scale, same as the corresponding figure in (a). Figures in different rows show MCNs with different  $n_B$ . (c) The diagram of MCN variants. “One-to-one” means the model only has one-to-one specific interactions. “All-same” means all the binding affinities are the same. “Constant-A” means the concentrations of all molecules  $A_i$  are determined by the environment. “Constant-B” means the concentrations of all molecules  $B_j$  are determined by the environment.

$2^2 = 4$  input tuples. Each output could be either 0 (low) or 1 (high), so there are  $2^4 = 16$  possible functions in total. Similarly, 3-input Boolean functions have input in  $\{0.01, 100\}$  and output in  $\{0, 1\}$ , and 2-input 3-quantized Boolean functions have input in  $\{0.01, 1, 100\}$  and output in  $\{0, 1\}$ . There are 16, 256, and 512 different Boolean functions in these task sets, respectively.

We restricted all  $K_{ij}$  and  $B_j^T$  between  $10^{-4}$  and  $10^4$ , and all  $W_{ij}$  and  $b$  between  $-10$  and  $10$ , to make the parameters close to biological or implementable scenarios. To better accommodate these Boolean classification tasks, we add a sigmoid function layer at the end of every model. Sigmoidlike functions can be easily implemented in biology, such as the Hill function-type response, except for their different input ranges. In this study, when the output is constrained to be non-negative, we set the last layer of the model as a Hill function with coefficient = 1. All these parameters were optimized to minimize the crossentropy loss between the output and the target. We trained each model several times independently and chose the best result for further analysis. We considered the fit

successful if the discretized output is the same as the target function. We visualized the output on a  $10 \times 10$  grid within the range of inputs at the logarithmic scale to investigate the computation pattern [Fig. 2(b)].

We selected a linear model and a multilayer perceptron (MLP) as the baseline model. The linear model only contains one linear layer of  $Y = \sum_i W_i A_i^T + b$ , which describes the computation directly driven by inputs  $A_i^T$  without any intermediate processing. The MLP is the most simple ANN which consists of one hidden linear layer including two nodes with sigmoid activation. The outputs of  $Y$  of these models were also processed by a sigmoid layer. As shown in Fig. 3, the linear model can only fit linear separable functions, while the MLP can fit more functions because of its nonlinear activation.

By contrast, we found that MCNs show great performance on these tasks (Fig. 3). MCNs with only one type of  $B$  ( $n_B = 1$ ), though a bit weaker than the linear model, can already fit some linear inseparable functions such as XOR. MCNs with  $n_B = 2$  can fit all 2-input Boolean functions (100%), nearly all 3-input Boolean functions (98%), and more than half of 2-input 3-quantized functions (67%). Linear inseparable functions like 2-input XOR and XNOR can be fitted. This result significantly outperforms the linear model and has a similar performance to the MLP, demonstrating that computational capacity gains from the competition layers. MCNs with  $n_B = 3$  can fit even more functions, about 100%, 100%, and 91%, respectively. The performance of MCNs increases rapidly with  $n_B$ , corroborating the findings in [14]. While MCNs do not contain a nonlinear “activation function” in the machine learning sense, MCNs are still able to fit nonlinear target functions, because competition layers effectively implement nonlinear interactions between inputs. All the results suggested the high computational capacity of MCNs in dealing with discrete decision-making tasks, which is particularly evident when facing linear inseparable functions.

#### IV. PROMISCUOUS BINDING AND LIMITED AMOUNTS OF RESOURCES ARE CRUCIAL FOR COMPUTATIONAL CAPACITY

As mentioned above, promiscuous binding coupled with limited amounts leads to molecular competition. We wondered whether the computational capabilities of MCNs are endowed by these characteristics. We proposed a model variant without promiscuous binding named “one-to-one MCN” where a type of molecule  $A$  only specifically binds with a type of molecule  $B$ . The competition layer of the one-to-one MCN could be regarded as a nonlinear activation layer based on the molecular titration effect [32] without crosstalk. We also proposed another model variant with homogeneous promiscuous binding named “all-same MCN” where all the promiscuous binding affinities are the same without any specificity, which, in other words, means that  $W_{ij}$  is independent from both  $i$  and  $j$ . We investigated the performance of these MCN variants with the same method (Fig. 3). The one-to-one MCNs and all-same MCNs just performed exactly the same as the linear model for fitting 2-input and 3-input Boolean functions. They are slightly different in 2-input 3-quantized functions, where the

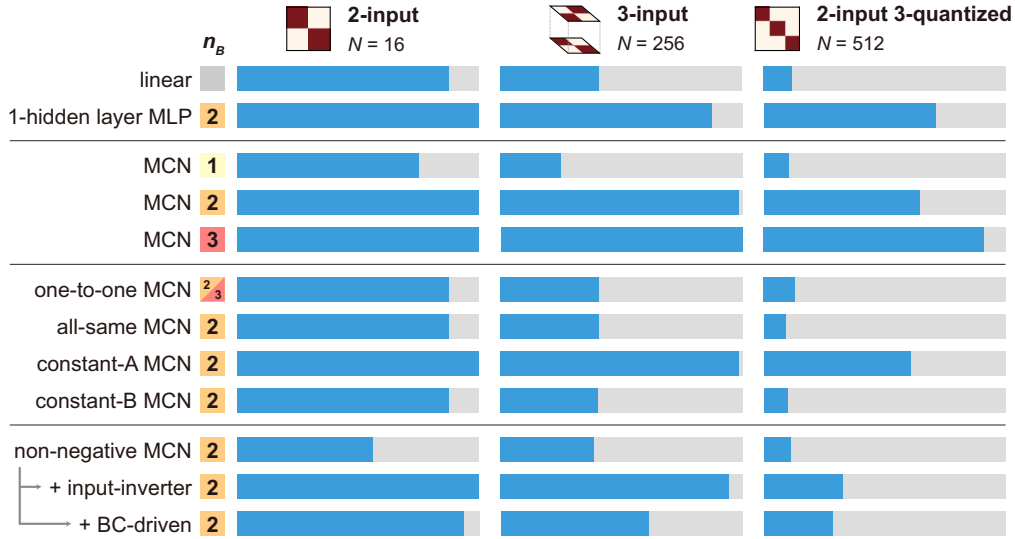


FIG. 3. The number of perfectly fitted functions of different models in different tasks. The blue part represents the proportion of perfectly fitted functions in this model. For the 1-hidden layer MLP,  $n_B$  denotes the number of nodes in the hidden layer. For the one-to-one MCN,  $n_B$  is determined by the number of inputs.  $N$  denotes the total number of functions. The exact numbers are shown in Supplemental Table 1 [26].

one-to-one MCNs could fit a little more than the linear model, but the all-same MCNs can fit less.

We further investigated MCNs with unlimited amounts of molecules. We considered a scenario where molecule  $A$  has unlimited amounts, e.g.,  $A$  is an extracellular ligand, and its concentration is only determined by the environment. We set  $[A_i] = A_i^T$  in this model and referred to it as a “constant- $A$  MCN:”

$$[C_{ij}] = K_{ij}[A_i][B_j] = \frac{K_{ij}A_i^T B_j^T}{1 + \sum_i K_{ij}A_i^T}. \quad (7)$$

Likewise, if molecule  $B$  has unlimited amounts, we set  $[B_j] = B_j^T$  and referred to it as a “constant- $B$  MCN.” In a constant- $B$  MCN, both  $[A_i]$  and  $[C_{ij}]$  are directly proportional to the input  $A_i$ , and the output  $Y$  is merely a linear combination of inputs  $A_i^T$ :

$$[C_{ij}] = K_{ij}[A_i][B_j] = K_{ij} \frac{1}{1 + \sum_j K_{ij}B_j^T} A_i^T B_j^T = \text{linear}(A_i^T). \quad (8)$$

As shown in Fig. 3, the constant- $A$  MCNs exhibited great performance across all tasks, only marginally worse than the original MCNs. It is similar to a previous conclusion that many-to-many protein interaction networks with the constant- $A$  assumption retain good behaviors [13]. The constant- $B$  MCNs performed just like the linear model with no surprises. All these results suggested that promiscuous binding with sophisticated specificity and limited amounts of resources are necessary for complex computation in MCNs.

## V. MCNS WITH STRONG BIOLOGICAL CONSTRAINTS RETAIN A PORTION OF COMPUTATIONAL CAPACITY

There are sometimes realistic constraints in biological networks. For instance, some competition scenarios may consist of molecules that drive the downstream response in the same

trend [8,15], where inhibition always occurs through competition with activating molecules. In this assumption, the linear layer weights  $W_{ij}$  in MCNs should be non-negative (non-negative MCNs). This constraint significantly reduces the computational capabilities of MCNs. When all inputs  $A_i^T$  are low, the equilibrium concentrations  $[C_{ij}]$  must be low, and the non-negative weights will result in a low output. As a result, the model theoretically fits at most half of the Boolean functions. In practice, the model fits nine 2-input Boolean functions and 99 3-input Boolean functions (Fig. 3).

The constraint can be compensated by slightly modifying the model structure. The input  $A_i$  can be inverted by other biological processes before joining the competition, in which case the non-negative MCNs can fit all 16 2-input functions and 242 3-input functions (Fig. 3). The resource  $B$  can also drive downstream signals in some other biological systems. In this case, when all  $A_i^T$  are low,  $[B_j] \approx B_j$  and has the ability to drive a high output. Such  $B$ ,  $C$ -driven non-negative MCNs can fit 15 2-input functions and 156 3-input functions, exhibiting a significant improvement compared to the  $C$ -driven non-negative MCNs (Fig. 3).

## VI. ROBUSTNESS OF MCNS WITH ALTERING AMOUNTS OF RESOURCES

Concentrations of molecular species in biological systems may show great variation among different cells due to intrinsic and extrinsic noise. Here, we explored whether the computational capabilities of MCNs change when the total amount of molecule  $B$  is altered. As shown in Fig. 4(a), most MCNs can preserve the performance with about 20% multiplicative noise. MCNs are more sensitive in decreasing  $B^T$  compared with increasing  $B^T$ , and the complex functions are more sensitive compared with simple functions. It reveals that MCNs showed fairly good noise resistance when performing Boolean operations, corroborating the findings in [14].

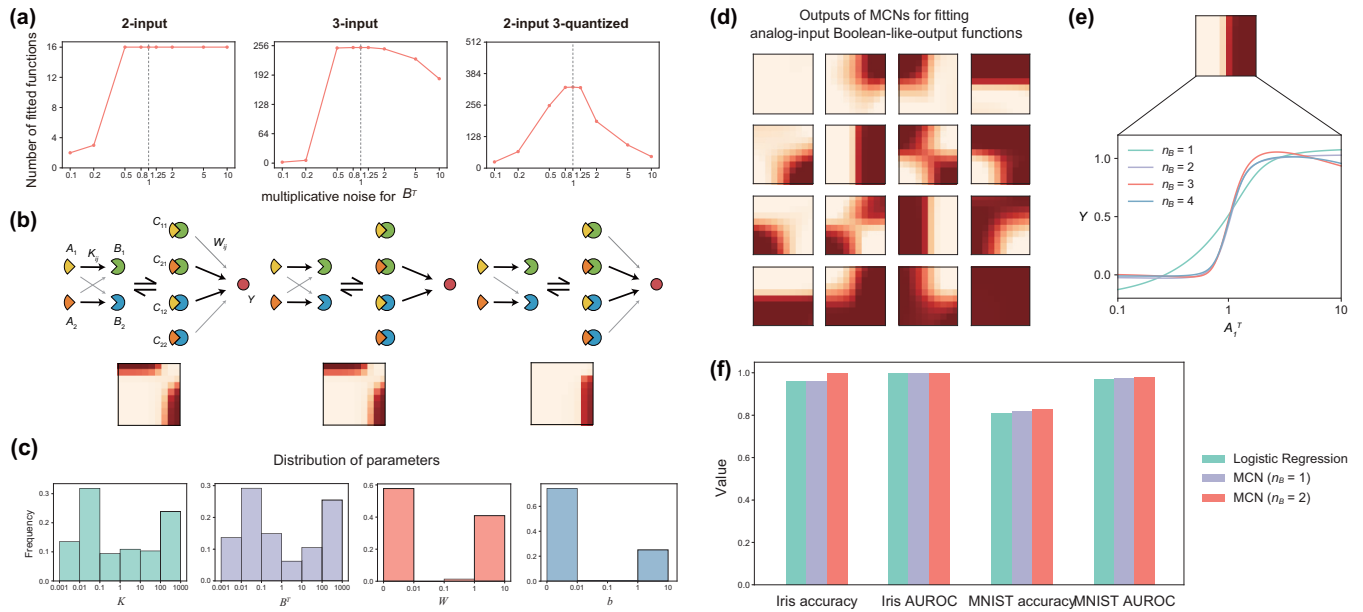


FIG. 4. (a) The robustness of MCNs with altering  $B^T$ . (b) Parameters and model outputs of  $n_B = 2$ , C-driven, and non-negative weight MCNs that fit the XOR function. Black lines represent strong interactions and gray lines represent weak interactions. Left: no modification; middle:  $K_{12}$  set as zero; right:  $K_{21}$  set as zero. (c) Parameter distributions of  $n_B = 3$ , C-driven, and non-negative weight MCNs that fit all 3-input Boolean function. (d) Visualization of MCN outputs trained for fitting analog-input Boolean-like-output functions. (e) Visualization of a sharp dose-response curve of (d). (f) Performance of models on multiclass classification tasks.

## VII. WEAK INTERACTIONS BETWEEN COMPETITORS AND RESOURCES ARE FUNCTIONAL IN MCNS

Weak interactions are widespread in biological networks. Though they are usually regarded as the result of off-target effects, several recent studies have demonstrated that these weak interactions have specific biological functions [4,33]. We wonder whether the weak interactions between competitors and resources are functional in MCNs. Here, we focused on the parameter settings of the non-negative, C-driven MCN with  $n_B = 2$ . We illustrated the parameters of the MCN which fits the XOR function [Fig. 4(b) left]. We found that  $K_{12}$  and  $K_{21}$ , which drive the production of  $C_{12}$  and  $C_{21}$ , respectively, are quite low. Meanwhile, both  $C_{12}$  and  $C_{21}$  greatly contribute to the output  $Y$  (high  $W_{12}$  and  $W_{21}$ ). This corroborates a previous discovery that the anticorrelation between the binding affinity and the activity to drive downstream signals can benefit the computational power [10]. We then investigated the role of these weak interactions by setting them as zero. When setting both  $W_{11}$  and  $W_{22}$  as zero, the model could still fit the XOR function [Fig. 4(b) middle], but when setting  $K_{21}$  as zero, the model failed to fit XOR anymore [Fig. 4(b) right].

We also analyzed the distribution of parameters in all MCNs that successfully fit any 3-input Boolean function [Fig. 4(c)]. We found that about 60%  $W_{ij}$  are exactly zero, while  $K_{ij}$  and  $B_j^T$  are more widely distributed. The results indicated that the linear layer is always sparse, while the competition layer is not. We then set the minimum  $K_{ij}$  as zero in every successfully fitted MCN. We found that 21% (21/99) of these MCNs cannot keep their functions anymore for fitting 3-input Boolean functions. These findings indicated weak interactions in the competition layer are common and functional in MCNs.

## VIII. MCNS CAN FIT ANALOG-INPUT FUNCTIONS WITH CLEAR AND ACCURATE BOUNDARIES

In the above sections, we only focused on binarized outputs corresponding to binarized or ternarized inputs. However, biological systems usually employ analog information processing, because molecular concentrations change continuously [34,35]. It is necessary to examine how MCNs perform under the requirements of more continuous inputs and more precise outputs. We followed the same method we used to train 2-input Boolean-like functions, with the only difference being that we generated  $10 \times 10$  grid points for training instead of only four endpoints. As shown in Fig. 4(d), MCNs with  $n_B = 2$  can fit all 2-input analog-input Boolean-like-output functions well. With more training samples, the model outputs are more similar to the target functions, with more clear and accurate boundaries.

The clear boundaries are consistent with previous studies which demonstrated that competition can induce ultrasensitivity in dose-response curves [4,32,36,37]. Here, we further investigated how sharp the transition boundary can be, generated by MCNs. As shown in Fig. 4(e), MCNs with  $n_B = 2$  can generate dose-response curves with Hill coefficients near six, and larger  $n_B$  cannot contribute more to the ultrasensitivity. The result showed that MCNs can be used to generate analogous patterns and revealed the upper bound of the ultrasensitivity that MCNs can achieve.

## IX. MCNS ARE CAPABLE OF PERFORMING CLASSIFICATION TASKS

We further explored the performance of MCNs in performing multiclass classification tasks. We applied MCNs to the

Iris dataset [38] and the MNIST dataset [39]. Each type of molecule  $A$  corresponds to one input feature, and each type of molecule  $Y$  corresponds to one class. Thus, MCNs for the Iris dataset have  $n_A = 4$  and  $n_Y = 3$ , while MCNs for the MNIST dataset have  $n_A = 784$  and  $n_Y = 10$ . The training objective is to maximize the output of the  $Y$  node corresponding to the correct category while minimizing the output of the other  $Y$  nodes. The inputs were normalized and transformed to the logarithmic scale. We split each dataset into training and test subsets. Specifically, for the Iris dataset, which contains 150 samples, we selected 100 for training. For the MNIST dataset, which contains 60 000 samples, we used 1000 for training. With these settings, MCNs with  $n_B = 2$  achieved both accuracy and AUROC close to 1.0 on the Iris dataset, and an accuracy of 0.830 and an AUROC of 0.978 on the MNIST dataset [Fig. 4(f) and Table 2 in the Supplemental Material [26]]. The performance of MCNs is slightly better than that of the classical logistic regression model. These results indicate that MCNs are capable of performing multiclass classification tasks.

## X. DISCUSSION

This study explored the computational capabilities of molecular competition networks using a machine learning optimization method. Our findings confirmed the computational capacity of competition networks and identify critical terms for competition computation. Biological systems, constrained by evolutionary pressures and resource limitations, inherently exhibit promiscuous interactions, thus making competition an inevitable phenomenon [40–42]. We propose that rather than being a detrimental factor, competition within promiscuous networks could act as an effective mechanism for cellular information processing.

Influenced by the modular design concept of electronic circuits, synthetic biology also uses basic modules to build complex genetic circuits. This methodology necessitates seven gates and 55 biobricks to assemble a 3-input consensus circuit [43]. Such complex hierarchical structures with cascading modules inevitably lead to more competition and crosstalk [44]. In contrast, MCNs with only two competitors ( $n_B = 2$ ) can execute all 3-input Boolean functions. Notably, MCNs consider and utilize the inherent competition. We believe that leveraging competition in gene circuit design could significantly advance synthetic biology. With the rapid development of AI-assisted design of DNA, RNA, and protein [45,46], it will be feasible

to realize optimized MCNs through synthetic biology techniques.

We supposed that MCNs could be also conceptualized as a generalized network structure for *in silico* applications. The restricted Boltzmann machine (RBM), which utilizes a bipartite graph structure similar to MCNs, is a well-established artificial neural network model that computes the probability distribution of each node based on “energy.” Analogously, MCNs, as natural systems, determine the probability distribution of each molecule according to the energies associated with all chemical reactions. Consequently, we hypothesize that MCNs could match or surpass the efficacy of RBMs in machine-learning applications. We assessed the performance of MCNs on standard machine learning tasks, such as the classification of the Iris and MNIST datasets. The results, detailed in the Supplemental Material [26], indicate that MCNs demonstrate robust performance in these contexts.

Different from traditional methods which explore the functionality of biological systems by assigning parameters randomly or based on prior knowledge, our machine learning-based optimization method first hypothesizes what function the networks behave, and then optimizes parameters to achieve the goal. This approach can also be easily applied in synthetic gene circuit design where a desired function comes first and then the parameters are optimized. Besides, it is worth calculating the equilibrium constants  $K_{ij}$  in natural MCNs as well as their changes in the evolutionary process and comparing them with the parameters optimized by machine learning to know whether real biological systems employ similar optimizing approaches to achieve certain information processing behaviors. It would be also interesting to further investigate and optimize more characteristics of MCNs by this method, such as dynamic behaviors, energy consumption, and robustness. Last but not least, in this study, we introduced a linear layer to simplify the relationship between the components in the competition layer and the output. We believe that an MCN cooperating with other network structures, or another MCN, may produce more complex results, which can be further explored in the future.

## ACKNOWLEDGMENTS

The work was supported by the National Natural Science Foundation of China (Grants No. 62250007, No. 62225307, No. 62103227, No. 62373210, and No. 61721003), and the National Key Research and Development Program of China (Grant No. 2020YFA0906900).

- [1] P. Nurse, Life, logic and information, *Nature (London)* **454**, 424 (2008).
- [2] G. H. Wadhams and J. P. Armitage, Making sense of it all: Bacterial chemotaxis, *Nat. Rev. Mol. Cell Biol.* **5**, 1024 (2004).
- [3] P. Li and M. B. Elowitz, Communication codes in developmental signaling pathways, *Development* **146**, dev170977 (2019).
- [4] L. Wei, Y. Yuan, T. Hu, S. Li, T. Cheng, J. Lei, Z. Xie, M. Q. Zhang, and X. Wang, Regulation by competition: A hidden layer of gene regulatory network, *Quant. Biol.* **7**, 110 (2019).
- [5] T. D. Mueller and J. Nickel, Promiscuity and specificity in BMP receptor activation, *FEBS Lett.* **586**, 1846 (2012).
- [6] P. J. Murray, The JAK-STAT signaling pathway: Input and output integration, *J. Immunol.* **178**, 2623 (2007).
- [7] B. Schmierer and C. S. Hill, TGF $\beta$ -SMAD signal transduction: molecular specificity and functional flexibility, *Nat. Rev. Mol. Cell Biol.* **8**, 970 (2007).
- [8] Y. E. Antebi, J. M. Linton, H. Klumpe, B. Bintu, M. Gong, C. Su, R. McCardell, and M. B. Elowitz, Combinatorial signal perception in the BMP pathway, *Cell* **170**, 1184 (2017).

- [9] H. E. Klumpe, M. A. Langley, J. M. Linton, C. J. Su, Y. E. Antebi, and M. B. Elowitz, The context-dependent, combinatorial logic of BMP signaling, *Cell Syst.* **13**, 388 (2022).
- [10] C. J. Su, A. Murugan, J. M. Linton, A. Yeluri, J. Bois, H. Klumpe, M. A. Langley, Y. E. Antebi, and M. B. Elowitz, Ligand-receptor promiscuity enables cellular addressing, *Cell Syst.* **13**, 408 (2022).
- [11] A. J. Genot, T. Fujii, and Y. Rondelez, Computing with competition in biochemical networks, *Phys. Rev. Lett.* **109**, 208102 (2012).
- [12] V. Singh and I. Nemenman, Universal properties of concentration sensing in large ligand-receptor networks, *Phys. Rev. Lett.* **124**, 028101 (2020).
- [13] H. E. Klumpe, J. Garcia-Ojalvo, M. B. Elowitz, and Y. E. Antebi, The computational capabilities of many-to-many protein interaction networks, *Cell Syst.* **14**, 430 (2023).
- [14] J. Parres-Gold, M. Levine, B. Emert, A. Stuart, and M. Elowitz, Principles of computation by competitive protein dimerization networks, *bioRxiv* (2023), doi:10.1101/2023.10.30.564854.
- [15] U. Ala, F. A. Karreth, C. Bosia, A. Pagnani, R. Taulli, V. Léopold, Y. Tay, P. Provero, R. Zecchina, and P. P. Pandolfi, Integrated transcriptional and competitive endogenous RNA networks are cross-regulated in permissive molecular environments, *Proc. Natl. Acad. Sci. USA* **110**, 7154 (2013).
- [16] N. Zhang, S. Ding, J. Zhang, and Y. Xue, An overview on restricted Boltzmann machines, *Neurocomputing* **275**, 1186 (2018).
- [17] K. Heinecke, A. Seher, W. Schmitz, T. D. Mueller, W. Sebald, and J. Nickel, Receptor oligomerization and beyond: A case study in bone morphogenetic proteins, *BMC Biol.* **7**, 59 (2009).
- [18] J. Gunawardena, Time-scale separation—Michaelis and Menten’s old idea, still bearing fruit, *FEBS J.* **281**, 473 (2014).
- [19] C. Ragan, M. Zuker, and M. A. Ragan, Quantitative prediction of Mirna-Mrna interaction based on equilibrium concentrations, *PLoS Comput. Biol.* **7**, e1001090 (2011).
- [20] W. Ma, A. Trusina, H. El-Samad, W. A. Lim, and C. Tang, Defining network topologies that can achieve biochemical adaptation, *Cell* **138**, 760 (2009).
- [21] M. Raissi, P. Perdikaris, and G. E. Karniadakis, Physics-informed neural networks: A deep learning framework for solving forward and inverse problems involving nonlinear partial differential equations, *J. Comput. Phys.* **378**, 686 (2019).
- [22] G. E. Karniadakis, I. G. Kevrekidis, L. Lu, P. Perdikaris, S. Wang, and L. Yang, Physics-informed machine learning, *Nat. Rev. Phys.* **3**, 422 (2021).
- [23] T. W. Hiscock, Adapting machine-learning algorithms to design gene circuits, *BMC Bioinf.* **20**, 214 (2019).
- [24] A. Yazdani, L. Lu, M. Raissi, and G. E. Karniadakis, Systems biology informed deep learning for inferring parameters and hidden dynamics, *PLoS Comput. Biol.* **16**, e1007575 (2020).
- [25] J. Shen, F. Liu, Y. Tu, and C. Tang, Finding gene network topologies for given biological function with recurrent neural network, *Nat. Commun.* **12**, 3125 (2021).
- [26] See Supplemental Material at <http://link.aps.org/supplemental/10.1103/PhysRevResearch.6.033208> for more details of the MCN model, the comparison between MCNs and the WTA structure, as well as Supplemental Table 1 and 2.
- [27] [https://github.com/maplecai/molecular\\_competition\\_network](https://github.com/maplecai/molecular_competition_network).
- [28] K. M. Cherry and L. Qian, Scaling up molecular pattern recognition with DNA-based winner-take-all neural networks, *Nature (London)* **559**, 370 (2018).
- [29] S. Okumura, G. Gines, N. Lobato-Dauzier, A. Baccouche, R. Deteix, T. Fujii, Y. Rondelez, and A. Genot, Nonlinear decision-making with enzymatic neural networks, *Nature (London)* **610**, 496 (2022).
- [30] R.-S. Wang, A. Saadatpour, and R. Albert, Boolean modeling in systems biology: An overview of methodology and applications, *Phys. Biol.* **9**, 055001 (2012).
- [31] N. Le Novère, Quantitative and logic modelling of molecular and gene networks, *Nat. Rev. Genet.* **16**, 146 (2015).
- [32] N. E. Buchler and M. Louis, Molecular titration and ultrasensitivity in regulatory networks, *J. Mol. Biol.* **384**, 1106 (2008).
- [33] L. Wei, S. Li, P. Zhang, T. Hu, M. Q. Zhang, Z. Xie, and X. Wang, Characterizing microrna-mediated modulation of gene expression noise and its effect on synthetic gene circuits, *Cell Rep.* **36**, 109573 (2021).
- [34] H. M. Sauro and K. Kim, It’s an analog world, *Nature (London)* **497**, 572 (2013).
- [35] R. Sarpeshkar, Analog synthetic biology, *Philos. Trans. R. Soc. A* **372**, 20130110 (2014).
- [36] N. E. Buchler and F. R. Cross, Protein sequestration generates a flexible ultrasensitive response in a genetic network, *Mol. Syst. Biol.* **5**, 272 (2009).
- [37] R. C. Brewster, F. M. Weinert, H. G. Garcia, D. Song, M. Rydenfelt, and R. Phillips, The transcription factor titration effect dictates level of gene expression, *Cell* **156**, 1312 (2014).
- [38] R. A. Fisher, The use of multiple measurements in taxonomic problems, *Ann. Eugenics* **7**, 179 (1936).
- [39] L. Deng, The MNIST database of handwritten digit images for machine learning research, *IEEE Signal Process. Mag.* **29**, 141 (2012).
- [40] M. A. Rowland and E. J. Deeds, Crosstalk and the evolution of specificity in two-component signaling, *Biophys. J.* **106**, 378a (2014).
- [41] S. D. Copley, An evolutionary biochemist’s perspective on promiscuity, *Trends Biochem. Sci.* **40**, 72 (2015).
- [42] T. B. Taylor, M. J. Shepherd, R. W. Jackson, and M. W. Silby, Natural selection on crosstalk between gene regulatory networks facilitates bacterial adaptation to novel environments, *Curr. Opin. Microbiol.* **67**, 102140 (2022).
- [43] A. A. Nielsen, B. S. Der, J. Shin, P. Vaidyanathan, V. Paralanov, E. A. Strychalski, D. Ross, D. Densmore, and C. A. Voigt, Genetic circuit design automation, *Science* **352**, aac7341 (2016).
- [44] K. Ilia and D. Del Vecchio, Squaring a circle: To what extent are traditional circuit analogies impeding synthetic biology? *GEN Biotechnol.* **1**, 150 (2022).
- [45] P.-S. Huang, S. E. Boyken, and D. Baker, The coming of age of *de novo* protein design, *Nature (London)* **537**, 320 (2016).
- [46] Z. Chen, S. E. Boyken, M. Jia, F. Busch, D. Flores-Solis, M. J. Bick, P. Lu, Z. L. VanAernum, A. Sahasrabudhe, R. A. Langan, S. Bermeo, T. J. Brunette, V. K. Mulligan, L. P. Carter, F. DiMaio, N. G. Sgourakis, V. H. Wysocki, and D. Baker, Programmable design of orthogonal protein heterodimers, *Nature (London)* **565**, 106 (2019).